Eur Radiol (2017) 27:3290–3299
DOI 10.1007/s00330-017-4739-6

CHEST

Ultralow dose CT for pulmonary nodule detection with chest x-ray equivalent dose – a prospective intra-individual comparative study

Michael Messerli[1,2] · Thomas Kluckert[2] · Meinhard Knitel[2] · Stephan Wälti[2,3] · Lotus Desbiolles[2] · Fabian Rengier[4] · René Warschkow[5] · Ralf W. Bauer[2] · Hatem Alkadhi[6] · Sebastian Leschka[2,6] · Simon Wildermuth[2]

Received: 6 July 2016 / Revised: 6 December 2016 / Accepted: 3 January 2017 / Published online: 16 January 2017

Abstract

Purpose To prospectively evaluate the accuracy of ultralow radiation dose CT of the chest with tin filtration at 100 kV for pulmonary nodule detection.

Materials and methods 202 consecutive patients undergoing clinically indicated chest CT (standard dose, 1.8 ± 0.7 mSv) were prospectively included and additionally scanned with an ultralow dose protocol (0.13 ± 0.01 mSv). Standard dose CT was read in consensus by two board-certified radiologists to determine the presence of lung nodules and served as standard of reference (SOR). Two radiologists assessed the presence of lung nodules and their locations on ultralow dose CT. Sensitivity and specificity of the ultralow dose protocol was compared against the SOR, including subgroup analyses of different nodule sizes and types. A mixed effects logistic regression was used to test for independent predictors for sensitivity of pulmonary nodule detection.

Results 425 nodules (mean diameter 3.7 ± 2.9 mm) were found on SOR. Overall sensitivity for nodule detection by ultralow dose CT was 91%. In multivariate analysis, nodule type, size and patients BMI were independent predictors for sensitivity ($p < 0.001$).

Conclusions Ultralow dose chest CT at 100 kV with spectral shaping enables a high sensitivity for the detection of pulmonary nodules at exposure levels comparable to plain film chest X-ray.

Keypoints

- *91% of all lung nodules were detected with ultralow dose CT*
- *Sensitivity for subsolid nodule detection is lower in ultralow dose CT (77.5%)*
- *The mean effective radiation dose in 202 patients was 0.13 mSv*
- *Ultralow dose CT seems to be feasible for lung cancer screening*

Keywords Pulmonary Nodule · Computed Tomography · Radiation Dosage · Image reconstruction · Lung cancer

✉ Michael Messerli
michael.messerli@usz.ch

[1] Department of Nuclear Medicine, University Hospital Zurich, University Zurich, Ramistrasse, Zurich, Switzerland

[2] Division of Radiology and Nuclear Medicine, Cantonal Hospital St. Gallen, St. Gallen, Switzerland

[3] Department of Radiology, CHU Sainte-Justine, University of Montreal, Montréal, Québec, Canada

[4] Department of Diagnostic and Interventional Radiology, University Hospital Heidelberg, Heidelberg, Germany

[5] Department of Surgery, Cantonal Hospital St. Gallen, St. Gallen, Switzerland

[6] Institute of Diagnostic and Interventional Radiology, University Hospital Zurich, University Zurich, Zurich, Switzerland

Abbreviations

ADMIRE	advanced modelled iterative reconstruction
CT	computed tomography
NLST	the National Lung Screening Trial
IR	iterative reconstruction

Introduction

Lung cancer is the most common cause of mortality from cancer leading to 1.59 million cancer deaths in 2012 [1]. In the United States a total of 224,390 new cases are estimated to

occur in 2016 of which almost 60% will be diagnosed in an advanced stage [2]. In contrast to the low overall 5-year survival of 15% [3], the 5-year relative survival rate without recurrence of non-small cell lung cancer can be as high as 80% when detected and adequately treated in an early stage [4, 5].

Numerous screening studies with computed tomography (CT) of the chest were initiated first in the United States in 2002-2004 (National Lung Screening Trial, NLST) [6] followed by programs in different European countries (e.g., ITALUNG, 2009 Italy [7]; NELSON-trial, 2011 Netherlands [8]). The first results of these screening programs suggested a reduced mortality among people at high risk [9]. The mean exposure in the NLST was 1.5 mSv per CT scan, and the study design included one CT in each of three consecutive years [6]. Taking into account further follow-up CT examinations of abnormal findings in some participants, this resulted in an estimated mean total radiation dose of 8 mSv over three years [10]. Since there has been a vibrant discussion of true and potential adverse biological effects of ionizing radiation as used in diagnostic radiology, various strategies have been developed to reduce patient exposure, including lowering the tube potential and tube current, automated exposure control, selective in-plane shielding and iterative image reconstruction (IR) [11–19].

Recently, the third-generation of dual-source CT was introduced having the feature of additional hardening of polychromatic X-ray spectra generated at 100 or 150 kV by means of a tin filter. This filter reduces the amount of low-energy photons that predominantly contribute to patient exposure but has only a little influence on the actual image information. The mean energy of the resulting spectrum is shifted to the higher energy levels and, hence, towards more penetrable photons leading to lower patient exposure without noticeable compromises in image quality [20].

Previous phantom studies showed promising results of this novel technique for the detection of pulmonary nodules at substantially reduced dose levels [21, 22].

The purpose of this study was to prospectively evaluate the accuracy of CT with tin filtration at 100 kV and an exposure level comparable to plain film chest X-ray for pulmonary nodule detection in a clinical setting without patient pre-selection.

Materials and methods

Study design

The patients included in this study are part of an ongoing prospective clinical single-center study (clinicaltrials.gov identifier NCT02468609) on ultralow radiation dose CT of the chest. The flow chart of the present study is given in Fig. 1. The local ethics committee approved the study. All patients gave written informed consent for an ultralow radiation dose CT that was conducted in addition to clinically indicated CT in the same session. No funding was received for the study. One author (R.W.B.) is on the speakers' bureau of Siemens Healthcare and was not in control of the study data. The study was conducted in compliance with ICH-GCP-rules and the Declaration of Helsinki.

Patients

Between February and June 2015, 272 consecutive patients (176 male, 96 female; mean age 62 years; range 18-90 years) who were referred to our department for a contrast-enhanced chest CT ($n = 228$) and non-enhanced chest CT (n = 44) were included.

Exclusion criteria for the study were (1) pregnancy and/or (2) age <18 years. A total of 22 patients were not included

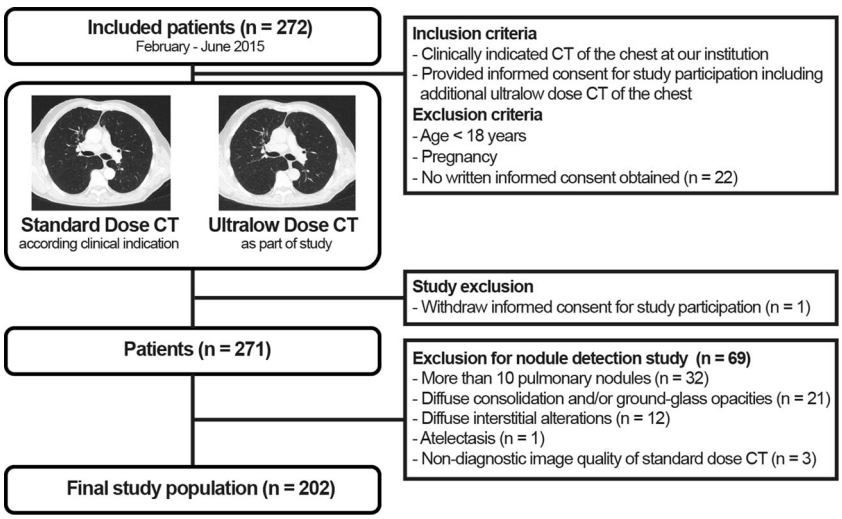

Fig. 1 Flow chart of study

because no written informed consent was obtained. One patient withdrew the informed consent and was, therefore, excluded. For the nodule detection study, a radiologist not involved in nodule readings (St.W., 5th year radiology resident) secondarily excluded cases where diagnostic nodule detection in standard dose CT was hampered by significant changes of lung parenchyma, i.e.: (1) diffuse consolidation and/or ground-glass opacities ($n = 21$), (2) diffuse interstitial alterations ($n = 12$), (3) atelectasis ($n = 1$), and (4) non-diagnostic image quality of standard dose CT ($n = 3$). Furthermore, patients with more than ten pulmonary nodules were excluded ($n = 32$).

Hence, the final study population consisted of 202 patients (130 male, 72 female; mean age 60 ± 14 years; age range 18-89 years). There were 130 men (mean age 59 ± 15 years; age range 18-89 years) and 72 women (mean age 62 ± 12 years; age range 33-89 years). Patient demographics are presented in Table 1.

CT examination protocol

All examinations were performed on a third-generation dual-source CT scanner (Somatom Force, Siemens Healthcare, Forchheim, Germany). A collimation of 96x0.6 mm and a slice acquisition of 192x0.6 mm by means of a z-flying focal spot were used. Gantry rotation time was 0.5 s at a pitch of 1.2, and all scans were conducted in inspiratory breath hold.

Patients were scanned with our institutional standard chest CT protocol, immediately followed by the ultralow dose scan comprising the same z-axis coverage. Standard dose CT was performed at reference settings of 110 kV and 50 quality reference mAs using automated attenuation-based tube current modulation (CAREDose4D; Siemens Healthcare) and automated attenuation-based tube potential selection (CAREkV; Siemens Healthcare; setting 7). Ultralow dose CT was performed at a fixed tube potential of 100 kV with a fixed tube current-time product of 70 mAs and additional tin filtration of the X-ray beam, resulting in a $CTDI_{vol}$ of 0.24 mGy (Table 2). Effective dose was calculated by multiplying the dose length product with the conversion coefficient k of 0.014 mSv/mGycm [23]. Based on the effective diameter of the chest, size-specific dose estimates (SSDE) were calculated applying the size-specific conversion factor f_{size} from the AAPM Report 204 ($SSDE = f_{size} \times CDTI_{vol}$) [24].

Table 1 Patient demographics and indications for CT

Male/female	130 (64%)/72 (36%)
Age, years	60 ± 14 (18 - 89)
Weight, kg	77 ± 18 (40 - 150)
Height, m	1.71 ± 0.1 (1.49 - 1.92)
BMI, kg/m^2	26.2 ± 5.3 (15.9 - 49)
Indications for CT	
Known or suspected tumour	132 (65%)
Suspected pulmonary infection	4 (2%)
Workup or follow-up of pulmonary nodule	19 (9%)
Workup or follow-up of pulmonary disease	31 (15%)
Abnormal chest X-ray findings	8 (4%)
Vascular[a]	6 (3%)
Thoracic skeleton assessment	2 (1%)
Performed CT study	
Contrast enhanced thoracic CT	169 (84%)
Non-enhanced thoracic CT	33 (16%)

CT computed tomography, BMI body mass index, presented as *n* (%) and mean ± SD (range)

[a] e.g., patients undergoing CT for exclusion of pulmonary embolism or follow-up of thoracic aortic aneurysm

Data reconstruction

CT images from standard dose and ultralow dose CT were reconstructed with advanced modelled iterative reconstruction (ADMIRE) as described in detail before [21] at a strength level of 3 out of 5 using a slice thickness of 2 mm with an increment of 1.6 mm and an edge-enhancing convolution kernel (Br64). The reconstructed field-of-view (FoV) was 400x400 mm^2. The image matrix was 512x512 pixels.

Image analyses were performed on a high-definition liquid crystal display monitor (BARCO; Medical Imaging Systems, Kortrijk, Belgium) using the picture archiving and communication system (ImpaxEE, VersionR20XVSU2; Agfa Healthcare N.V., Mortsel, Belgium) of our hospital. The two radiologists involved in the nodule detection were free to use all the capabilities of the picture archiving and communication system at their own discretion (e.g., maximum intensity projection images).

CT data analysis

Image noise

One blinded reader (L.D., 12 years of experience in radiology) who was not involved in any other image evaluation measured image noise of standard and ultralow dose CT scans in random order by placing a region of interest (ROI) in the trachea above the level of the carina representing the central scan FoV. The size of the ROI was 100 mm^2 and adjacent structures were avoided. Mean image noise was defined as the average of the standard deviation of the attenuation of air in three consecutive ROIs at different z-axis positions.

Subjective image quality

The axial images of both standard and ultralow dose CT were independently presented in random order to two readers (M.K.

Table 2 Scan and radiation dose parameters of study protocols

	Standard dose protocol	Ultralow dose protocol	*p*-value[a]
Tube potential (kVp)			<0.001
80	1[b]	--	
90	10[b]	--	
100	133[b]	202	
110	42[b]	--	
120	7[b]	--	
140	3[b]	--	
150	6[b]	--	
Tube current time product (mAs)	73.3 ± 28.2 (25.0 - 233.0)	70	
Automated tube current modulation	On	Off	
Automated tube voltage selection	On	Off	
Scan length, cm	34.4 ± 3.0 (26.4 - 43.1)	34.4 ± 3.0 (26.4 - 43.1)	1.000
$CTDI_{Vol}$, mGy	3.2 ± 1.2 (1.1 - 8.3)	0.24	<0.001
DLP, mGy-cm	126.5 ± 48.1 (45.9 - 346.8)	9.5 ± 0.7 (7.5 - 11.6)	<0.001
ED, mSv	1.8 ± 0.7 (0.64 - 4.9)	0.13 ± 0.01 (0.11 - 0.16)	<0.001
Effective diameter	30 ± 3 (22 - 39)	30 ± 3 (22 - 39)	1.000
SSDE, mGy	3.9 ± 1 (1.8 - 8.1)	0.3 ± 0.04 (0.2 - 0.4)	<0.001

CT computed tomography, $CTDI_{vol}$ volume CT dose index, DLP dose length product, ED effective dose, SSDE size-specific dose estimate, presented as *n* (%) and mean ± SD (range)

[a] Wilcoxon-test for paired non-parametric data

[b] *n* patients, based on reference settings of 110 kV and 50 quality reference mAs using automated attenuation-based tube current modulation and tube potential selection

and T.K., with 7 and 20 years of experience in radiology) who were blinded to all information regarding the patient and indication for CT. Images were initially presented with a window level of -600 HU and a width of 1200 HU; readers were allowed to modify the window width and level according to their preferences. Overall image quality of standard and ultralow dose CT scans was graded on a modified 5-point Likert scale as previously shown [19]: 1 = nondiagnostic image quality, strong artifacts, insufficient for diagnostic purposes score; 2 = severe artefacts with uncertainty about the evaluation; 3 = moderate artefacts with restricted assessment; 4 = slight artefacts with unrestricted diagnostic image evaluation possible; and 5 = excellent image quality, no artifacts. Scans with a quality score of 3 to 5 were considered diagnostic.

Standard of reference

To establish the standard of reference (SOR) the two board-certified radiologists (M.K. and T.K., with 7 and 20 years of experience in radiology) who evaluated subjective image quality read the datasets of standard dose CT ($n = 202$) by consensus in random order and blinded to clinical information. The radiologists included the lesions that met the following criteria: (1) rounded intrapulmonary opacities - nodules according the Fleischner Society [25], (2) diameter 1-25 mm, (3) solid, subsolid or calcified nodules, (4) pleura-based lesions when the center was intrapulmonary in round lesions or when the height was greater than the base in oval lesions as previously described [26]. The following lesions were excluded: (5) perifissural nodules according to de Hoop et al. [27], and (6) apical subpleural lesions when in linear continuity with the pleura. Each nodule was measured in the long-axis and was classified as solid, subsolid or calcified.

Detection of pulmonary nodules

In a second reading session the two readers who established the SOR evaluated the ultralow radiation dose CT studies ($n = 202$) and marked each nodule similarly to the SOR. The second reading was performed 12 weeks after the initial consensus reading to avoid recall bias. The datasets were shown in random order and readers were blinded to any patient information. Both readers performed the second reading session independently, and they were unaware of the markings of the other reader. After this second reading session, every marked nodule in the ultralow dose images was controlled in a side-by-side fashion with the marked nodules in the SOR by a third radiologist (M.M., fourth year radiology resident) not involved in any other image evaluation. In case of discrepancy of markings, a decision was made by consensus by three radiologists. All correctly detected lesions were classified as "true positive". Lesions indicated on ultralow dose CT, but not on SOR, were considered as "false positive". Lesions that

were not seen on ultralow dose CT, but seen on SOR, were considered as "false negative" lesions. For per-patient analyses CT scans with no lesions marked in either the ultralow dose CT or SOR were considered as "true negative" and served as negative control.

Statistical analysis

Statistical analyses were performed using the R statistical software (www.r-project.org). A two-sided p-value of <0.05 was considered statistically significant. Continuous data are expressed as mean ± standard deviation. Chi-Square statistics, Wilcoxon-tests for paired non-parametric data, and t-tests were used to compare proportions and continuous variables. Nodule detection was analysed in per-patient (i.e., presence or absence of pulmonary nodules per patient) and per-nodule analysis. Sensitivity and specificity of ultralow dose CT for detection of pulmonary nodules were determined along with 95% confidence intervals and compared by Chi-Square statistics using the standard dose CT as the standard of reference. For the per-nodule analysis, a mixed effects logistic regression was used to model the detection of pulmonary nodules as a binary outcome. The log odds of detection was modelled as a linear combination of the main effects of the predictor variables also including the patient identification number as a factorial random effects using the R package lmer [28]. The full model logistic regression was further elucidated by a backward variable selection procedure from the full model based on the Akaike's information criterion. P-values were computed by likelihood-ratio-tests and Wald-type confidence intervals were estimated.

Results

In standard dose CT a total of 425 nodules (254 solid; 71 subsolid; 100 calcified) with a mean diameter of 3.7 ± 2.9 mm (range 1-24 mm) were defined. Pulmonary nodules were found in 153 patients (76%), 49 patients (24%) had no nodules.

Image noise

Mean image noise for images of the standard dose protocol was 48 ± 7 HU. Image noise was significantly higher in ultralow dose images with an average noise of 65 ± 5 HU; $p < 0.001$.

Subjective image quality

Both readers rated the overall image quality to be diagnostically sufficient for all images of the ultralow radiation dose CT (Fig. 2). Subjective image quality for ultralow dose was rated lower compared to standard dose images by both readers ($p < 0.001$). Both readers rated subjective image quality

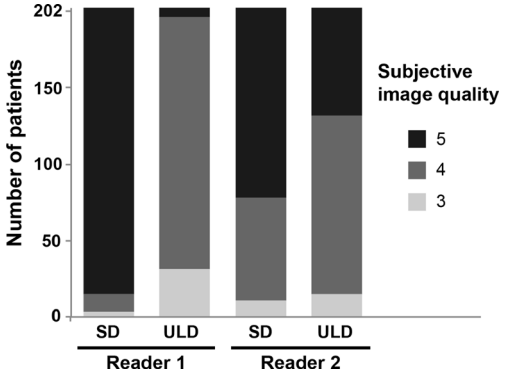

Fig. 2 Subjective image quality ratings of reader 1 and reader 2 for standard dose (SD) and ultralow dose (ULD) CT

significantly lower in patients with a BMI exceeding 30 kg/m^2 in ultralow dose CT ($p < 0.001$) but not in standard dose CT ($p > 0.05$).

Detection of pulmonary nodules

On per-patient analysis, sensitivity and specificity were 98.0% and 93.9%, on per-nodule analysis, overall sensitivity was 91.2% (Table 3). In solid, calcified, and subsolid nodules 243 of 254 (95.7%), 90 of 100 (90.0%), and 55 of 71 (77.7%) lesions were detected, respectively (Table 4). The 37 false negative lesions had a diameter of 1 mm in 8 (22%), 2 mm in 14 (38%), 3 mm in 12 (32%), 4 mm in 1 (3%), 5 mm in 1 (3%) and 7 mm in 1 (3%) of the nodules, respectively.

Table 3 Per-patient and per-nodule diagnostic performance of ultralow dose CT with standard dose CT as standard of reference

	All patients
Per-Patient Analysis[a]	
Number of patients	202
True positive	150
False negative	3
True negative	46
False positive	3
Sensitivity (95% CI)	98.0% (94.3 - 99.6%)
Specificity (95% CI)	93.9% (83.1 - 98.7%)
Per-Nodule Analysis	
Number of nodules	425[b]
True positive	388
False negative	37
Sensitivity (95% CI)	91.2% (88.2 - 93.8%)

CT computed tomography, CI confidence interval, presented as n (%) and mean ± SD (range)

[a] i.e., presence or absence of pulmonary nodules per patient

[b] additionally 16 false positive lesions

Table 4 Per-nodule diagnostic performance of ultralow dose CT with standard dose CT as standard of reference including different nodule types and sizes

	solid	calcified	subsolid
Number of nodules	254	100	71
Mean diameter, mm	4.4 ± 3.7 (1.0 - 24.0)	2.2 ± 1.0 (1.0 - 7.0)	3.3 ± 1.8 (1.0 - 10.0)
True positive, *n*	243	90	55
False negative, *n*	11	10	16
Sensitivity (95% CI)	95.7% (92.4 - 97.8%)	90% (82.4 - 95.1%)	77.5% (66.0 - 86.5%)
	<5 mm	5 - 7 mm	>7 mm
Number of nodules	334	70	21
Nodule type			
solid, *n*	179 (54%)	56 (80%)	19 (90%)
calcified, *n*	97 (29%)	3 (4%)	0 (0%)
subsolid, *n*	58 (17%)	11 (16%)	2 (10%)
True positive, *n*	299	68	21
False negative, *n*	35	2	0
Sensitivity (95% CI)	89.5% (85.7 - 92.6%)	97.1% (90.0 - 99.6%)	100% (83.9 - 100%)

CT computed tomography, CI confidence interval, presented as *n* (%) and mean ± SD (range)

Sensitivity of ultralow dose CT was significantly higher for greater nodule diameter, lower patients BMI, lower image noise, and solid and calcified nodules (Table 5). In multivariate analysis, nodule type, size and BMI were independent predictors for sensitivity (Figs. 3 and 4). For detection of a nodule sized ≥5 mm, the sensitivity was 97.3% across all nodule types compared to 92.0% for subsolid nodules. Across all nodules, the sensitivity was 92.6% and 84.9% in patients with a BMI of 25 kg/m^2 and 35 kg/m^2, respectively. When evaluating the

Table 5 Univariate and multivariate analysis of per-nodule diagnostic performance of ultralow dose CT with standard dose CT as standard of reference

		Univariate analysis				Multivariate analysis in logistic regression [d]			
						Full model		Variable selection model	
		Total (*n* = 425)	Detected (*n* = 388)	Not Detected (*n* = 37)	*p*-value	Odds ratio (95% CI)	*p* [e]	Odds ratio (95% CI)	*p* [e]
Nodule type	solid	254 (59.8%)	243 (62.6%)	11 (29.7%)	<0.001 [a]	reference	<0.001	reference	<0.001
	calcified	100 (23.5%)	90 (23.2%)	10 (27.0%)		0.83 (0.31-2.24)		0.76 (0.29-1.99)	
	subsolid	71 (16.7%)	55 (14.2%)	16 (43.2%)		0.17 (0.07-0.41)		0.17 (0.07-0.41)	
Nodule size	(mm)	3.7 ± 2.9	3.8 ± 3.0	2.4 ± 1.2	<0.001 [b]	1.93 (1.34-2.78)	<0.001	1.82 (1.28-2.58)	<0.001
Nodule localisation	right upper lobe	124 (29.2%)	112 (28.9%)	12 (32.4%)	0.812 [a]	reference	0.639	-	-
	middle lobe	45 (10.6%)	42 (10.8%)	3 (8.1%)		0.80 (0.19-3.32)		-	
	right lower lobe	96 (22.6%)	88 (22.7%)	8 (21.6%)		0.86 (0.31-2.39)		-	
	left upper lobe	69 (16.2%)	61 (15.7%)	8 (21.6%)		0.44 (0.15-1.27)		-	
	left lower lobe	91 (21.4%)	85 (21.9%)	6 (16.2%)		1.00 (0.32-3.09)		-	
Number of nodules per patient	n	3.9 ± 2.1	3.9 ± 2.2	3.9 ± 2.0	0.900 [b]	1.04 (0.86-1.26)	0.660	-	-
Age	years	62.4 ± 13.4	62.4 ± 13.6	62.1 ± 10.2	0.855 [b]	1.00 (0.97-1.02)	0.733	-	-
Gender	Male	291 (68.5%)	267 (68.8%)	24 (64.9%)	0.621 [c]	reference	0.935	-	-
	Female	134 (31.5%)	121 (31.2%)	13 (35.1%)		0.97 (0.43-2.17)		-	
BMI	kg/m^2	26.4 ± 5.4	26.2 ± 5.3	28.4 ± 6.0	0.035 [b]	0.93 (0.86-1.01)	0.084	0.91 (0.86-0.97)	0.006
Image Noise	HU	63.9 ± 5.7	63.7 ± 5.7	66.1 ± 5.3	0.012 [b]	0.95 (0.87-1.03)	0.223	-	-

CT computed tomography, BMI body mass index, HU Hounsfield units, odds ratio (95% confidence interval), *n* (%), mean ± SD (range)

[a] Monte-Carlo simulated Chi-squared test

[b] t-Test

[c] Chi-squared test

[d] Mixed effects logistic regression modeling the detection of nodes as a linear combination of fixed effect predictor variables and patient as random effects, as full model and after variable selection

[e] Likelihood-ratio-tests

nodules ≥5 mm ($n = 91$) the sensitivity was 98% and 97% in patients with a BMI of 25 kg/m^2 and 35 kg/m^2, respectively (Fig. 4).

Representative cases of standard dose and ultralow dose CT are given in Figs. 5 and 6.

Discussion

This study sought to evaluate the accuracy of an ultralow radiation dose CT protocol of the chest for nodule detection with additional hardening of a 100 kV source spectrum by a tin filter in combination with modern IR. For this purpose, we prospectively included a large number of consecutive patients undergoing standard dose CT of the chest for a variety of clinical indications and imaged them in addition with an ultralow dose CT protocol being associated with radiation dose values similar to plain film chest X-ray, which are on average 0.1 mSv for a posteroanterior and lateral study of the chest [29]. Our results indicate that although the subjective image quality is lower at this ultralow radiation dose, it is still considered diagnostic in all cases. The sensitivity of pulmonary nodule detection is high across all patients as well as in various sub-group analyses.

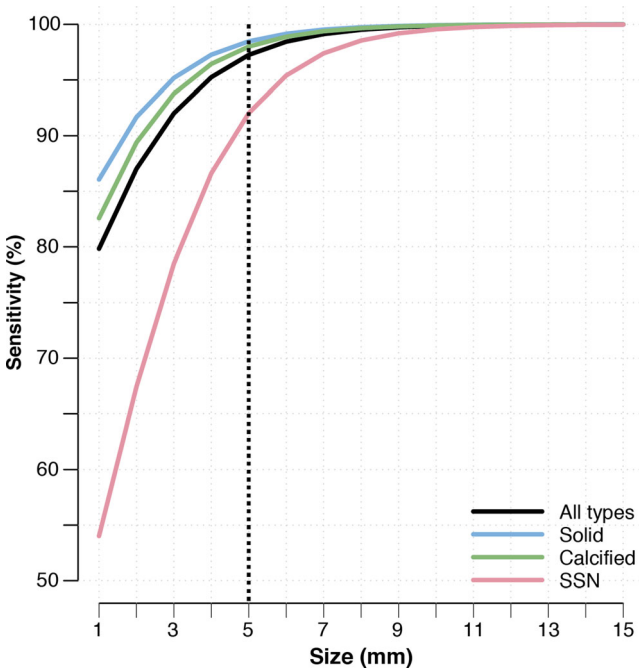

Fig. 3 Predicted sensitivity for pulmonary nodules in per-nodule analysis depending on type and size in mixed effects logistic regression analysis including all nodules ($n = 425$). Sensitivity increased for all types of nodules with increasing size of the nodule. The predicted sensitivity for subsolid pulmonary nodules (SSN) was lower for all sizes

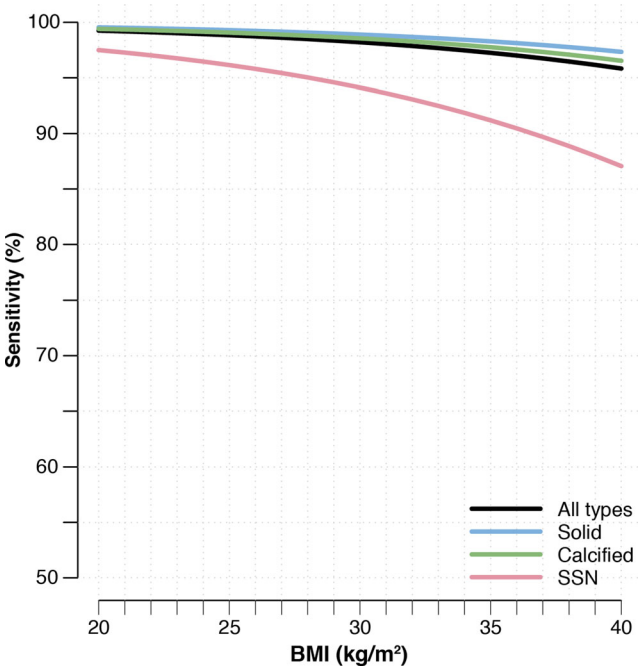

Fig. 4 Predicted sensitivity for pulmonary nodules in per-nodule analysis depending on type and body mass index (BMI) in mixed effects logistic regression analysis including all nodules ≥5 mm ($n = 91$). Sensitivity decreased for all types of nodules with increasing BMI. The predicted sensitivity for subsolid pulmonary nodules (SSN) was lower for all BMI values

The overall sensitivity per-nodule was 91%, being lower than the per-patient sensitivity of 98%. This is explained by the fact that the per-patient sensitivity indicates only whether or not a patient has pulmonary nodules. Regarding the lower per-nodule sensitivity we have to take into consideration that 35 of 37 (95%) of the false negative nodules were smaller than 5 mm. The risk for malignancy in small nodules with a diameter of <5 mm is very low with less than 1% even in a high risk population [30]. This is reflected in the guidelines for the management of pulmonary nodules of the British Thoracic Society (BTS) published in 2015 [31], which do not recommend routine nodule follow-up for nodules <5 mm in maximum diameter.

Recently, multiple lung cancer screening programs with CT of the chest have been started in different countries [6–8]. First results of the NLST suggested reduced mortality by 20% among people at high risk [9]. However, because of the high cumulative dose due to repetitive screening CT examinations the basic concept of ALARA ("as low as reasonably achievable") regarding radiation is of utmost importance. Interestingly, what was regarded a "low dose" examination in the NLST 14 years ago, is meanwhile a "standard dose" examination, given the fact that due to rapid technological developments in CT the average exposure of our standard protocol which utilizes automated mAs and kV adaption as well as IR results in 1.8 mSv only. Indeed, the automatically

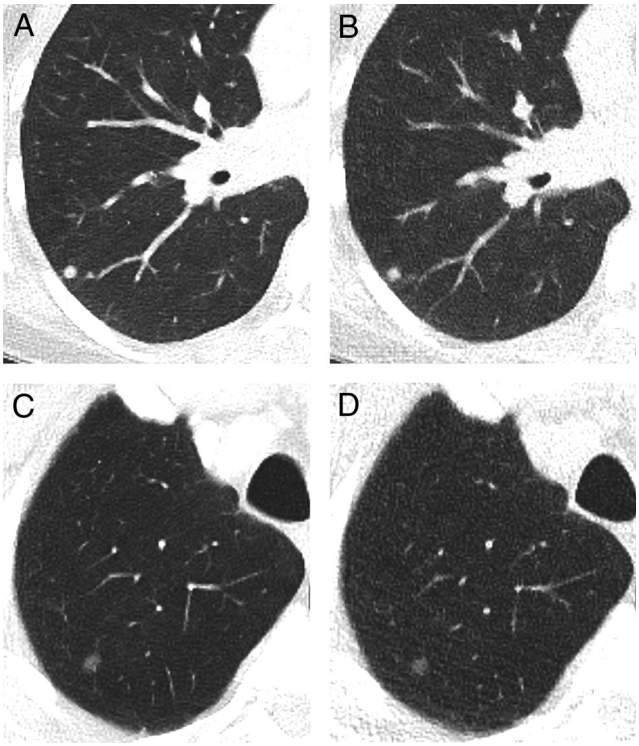

Fig. 5 Representative transverse CT sections of the lung in a 33-year-old woman with a body mass index of 23.6 kg/m2 scanned with standard dose (A) at 110 kVp and 38 mAs (effective dose, 1.1 mSv; size-specific dose estimate, 3.09 mGy) and ultralow dose (B) at 100 kVp and 70 mAs (effective dose, 0.14 mSv; size-specific dose estimate, 0.37 mGy). The solid pulmonary nodule in the right lower lobe was detected in ultralow dose CT by both readers (i.e., true positive finding). Representative transverse CT sections of the lung in a 79-year-old man with a body mass index of 24.9 kg/m2 scanned with standard dose (C) at 100 kVp and 62 mAs (effective dose, 1.33 mSv; size-specific dose estimate, 3.1 mGy) and ultralow dose (D) at 100 kVp and 70 mAs (effective dose, 0.13 mSv; size-specific dose estimate, 0.3 mGy). The subsolid pulmonary nodule in the right upper lobe was detected in ultralow dose CT by both readers (i.e. true positive finding)

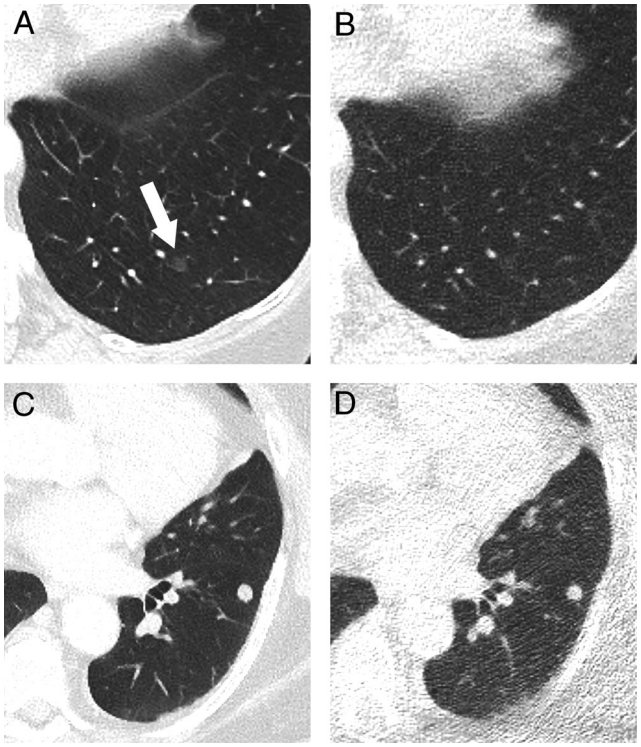

Fig. 6 Representative transverse CT sections of the lung in a 75-year-old woman with a body mass index of 24.4 kg/m2 scanned with standard dose (A) at 100 kVp and 54 mAs (effective dose, 1.09 mSv; size-specific dose estimate, 3.13 mGy) and ultralow dose (B) at 100 kVp and 70 mAs (effective dose, 0.12 mSv; size-specific dose estimate, 0.34 mGy). The subsolid pulmonary nodule in the left lower lobe (arrow) was not detected by either of the reader in ultralow dose CT (i.e., false negative finding). Representative transverse CT sections of the lung in a 75-year-old woman with a body mass index of 42.8 kg/m2 scanned with standard dose (C) at 110 kVp and 142 mAs (effective dose, 4.13 mSv; size-specific dose estimate, 6.86 mGy) and ultralow dose (D) at 100 kVp and 70 mAs (effective dose, 0.13 mSv; size-specific dose estimate, 0.22 mGy). Note the markedly increased image noise in the ultralow dose CT scan. In spite of the image noise the solid pulmonary nodule in the left lower lobe was detected in ultralow dose CT by both readers (i.e., true positive finding)

selected kV settings in our standard dose protocol were in a wide range. However, the effect of photon starvation and beam hardening on nodule appearance should be negligible in a high-contrast environment as the lung, especially as the automated adaption of tube potential went hand in hand with concurrent adaption of the tube current as by the manufacturer's default. Consequently, it is very unlikely that a nodule was missed on standard dose CT due to the mentioned physical effects or general "underdosing". Hence, we do not see a physical reason for a potential bias, and we believe that all included standard dose scans can well serve as a standard of reference. The "low dose" protocol used in the NLST had an average dose of 1.5 mSv per scan [6], being substantially higher compared to 0.13 mSv achieved with our ultralow dose protocol. As our results underline, still we benefit from the advantages of a cross-sectional imaging modality. The application of our protocol in a screening setting would result in an estimated mean total dose of 0.39 mSv over three years when applied according the NSLT study design. Thus, when taking into account that every citizen in Europe is exposed to 2 - 7 mSv of background radiation per year [32], the amount of extra radiation exposure from our study protocol seems relatively small and is most likely outweighed by the beneficial effects from screening targeting a high risk population only.

Regarding diagnostic performance criteria for screening purposes, a recent study systematically investigated criteria for screening mammography [33], and defined the performance levels that are minimally acceptable for sensitivity and specificity as ≥80% and ≥85%, respectively. These values are well exceled in this study with a sensitivity of 98% and specificity of 94%. Our results are in contrast to a recent study that investigated the same CT equipment as used in our study with ADMIRE and tin filtration for detection of pulmonary infection and nodules [34]. Interestingly, the reported

sensitivity of 71% was substantially lower. The authors did not further specify the mean size or category of nodules, which might be a potential reason for lower accuracy. Further, their used protocol was slightly different with a $CTDI_{vol}$ of 0.07 mGy as opposed to 0.24 mGy in our protocol resulting in a lower mean DLP of 4.9 mGycm as opposed to 9.5 mGycm. This may reflect a source of impaired image quality and, hence, hampered nodule detection.

In our study the sensitivity for the detection of subsolid nodules in ultralow dose CT was lower with 78% compared to 96% for solid nodules, which has been described before by Nagatani et al. [26]. However, when evaluating the relevant subsolid nodules with a diameter of ≥5 mm, which might need follow up according the recent recommendations of the BTS [31], the sensitivity was markedly higher with 11 of 13 detected nodules (sensitivity 85%). Further studies with a greater number of subsolid nodules are required to evaluate the value of this CT protocol for this subgroup of nodules.

Obesity is a known source for impaired image quality in CT due to photon starvation artifacts and increased image noise [35] which leads to degradation of image quality. In our study increased BMI was confirmed as an independent negative predictor for sensitivity. However, even in severely obese patients the sensitivity for all nodule types still was high (for example, 85% with a BMI of 35 kg/m^2). Nevertheless, we recommend the ultralow dose protocol to be used preferably in patients with a BMI <35 kg/m^2. Future studies may address the use of spectral shaping and dose optimization in obese patients to further refine ultralow dose protocols. Following the results of our study, we have implemented the ultralow dose protocol in our clinical routine and use it as a standard protocol for nodule follow-up in patients with BMI <35 kg/m^2. Furthermore, we now routinely use the ultralow dose protocol for annual screening in patients with a history of asbestos exposure who are referred by occupational health insurance.

Our study has some limitations. First, we have to acknowledge the inherent limitations of in vivo studies on pulmonary nodule detection performance because no gold standard is available, only a reference standard, which was represented by standard dose CT and consensus reading. Second, we did not reconstruct images with FBP or varying strength levels of IR to test for potential influence of reconstruction parameters on nodule detectability. Third, we did not test the inter- and intraobserver variability of readers for detecting pulmonary nodules on the ultralow dose CT protocol. However, we strongly encourage further studies to assess potential differences in agreement of nodule detection in standard dose compared to ultralow dose CT, ideally with multiple readers of various expertise levels so that potentially meaningful variability can be obtained and reported.

In conclusion, our study suggests that dose levels of chest CT for the detection of pulmonary nodules can be lowered down to 0.13 mSv when using 100 kV with spectral shaping in combination with latest IR technique while image quality remains diagnostic and sensitivity remains high. The combination of chest X-ray-like exposure levels, diagnostically sufficient image quality and high sensitivity for nodule detection makes the ultralow dose CT protocol potentially suitable for lung cancer screening.

Compliance with ethical standards

Guarantor The scientific guarantor of this publication is Michael Messerli.

Conflict of interest The authors of this manuscript declare relationships with the following companies: MD Ralf W. Bauer is on the speakers' bureau of Siemens Healthcare AG.

Funding The authors state that this work has not received any funding.

Statistics and biometry One of the authors has significant statistical expertise.

Informed consent Written informed consent was obtained from all subjects (patients) in this study.

Ethical approval Institutional Review Board approval was obtained.

Methodology
- prospective
- diagnostic or prognostic study
- performed at one institution

References

1. Ferlay J, Soerjomataram I, Dikshit R et al (2015) Cancer incidence and mortality worldwide: sources, methods and major patterns in GLOBOCAN 2012. Int J Cancer 136:E359–E386
2. Siegel RL, Miller KD, Jemal A (2016) Cancer statistics, 2016. CA Cancer J Clin 66:7–30
3. Janssen-Heijnen ML, Coebergh JW (2001) Trends in incidence and prognosis of the histological subtypes of lung cancer in North America, Australia, New Zealand and Europe. Lung Cancer 31: 123–137
4. Carr SR, Schuchert MJ, Pennathur A et al (2012) Impact of tumor size on outcomes after anatomic lung resection for stage 1A non-small cell lung cancer based on the current staging system. J Thorac Cardiovasc Surg 143:390–397
5. Cerfolio RJ, Bryant AS (2009) Survival of patients with true pathologic stage I non-small cell lung cancer. Ann Thorac Surg 88:917–922, discussion 922-913
6. National Lung Screening Trial Research T, Aberle DR, Berg CD et al (2011) The National Lung Screening Trial: overview and study design. Radiology 258:243–253
7. Picozzi G, Paci E, Lopez Pegna A et al (2005) Screening of lung cancer with low dose spiral CT: results of a three year pilot study and design of the randomised controlled trial "Italung-CT". Radiol Med 109:17–26
8. Ru Zhao Y, Xie X, de Koning HJ, Mali WP, Vliegenthart R, Oudkerk M (2011) NELSON lung cancer screening study. Cancer Imaging 11 Spec No A:S79-84

9. National Lung Screening Trial Research T, Aberle DR, Adams AM et al (2011) Reduced lung-cancer mortality with low-dose computed tomographic screening. N Engl J Med 365:395–409
10. Bach PB, Mirkin JN, Oliver TK et al (2012) Benefits and harms of CT screening for lung cancer: a systematic review. JAMA 307: 2418–2429
11. Bankier AA, Tack D (2010) Dose reduction strategies for thoracic multidetector computed tomography: background, current issues, and recommendations. J Thorac Imaging 25:278–288
12. Kalender WA, Buchenau S, Deak P et al (2008) Technical approaches to the optimisation of CT. Phys Med 24:71–79
13. Baumueller S, Alkadhi H, Stolzmann P et al (2011) Computed tomography of the lung in the high-pitch mode: is breath holding still required? Invest Radiol 46:240–245
14. Christner JA, Zavaletta VA, Eusemann CD, Walz-Flannigan AI, McCollough CH (2010) Dose reduction in helical CT: dynamically adjustable z-axis X-ray beam collimation. AJR Am J Roentgenol 194:W49–W55
15. Paul NS, Blobel J, Prezelj E et al (2010) The reduction of image noise and streak artifact in the thoracic inlet during low dose and ultra-low dose thoracic CT. Phys Med Biol 55:1363–1380
16. Baumueller S, Winklehner A, Karlo C et al (2012) Low-dose CT of the lung: potential value of iterative reconstructions. Eur Radiol 22: 2597–2606
17. Kalra MK, Maher MM, Sahani DV et al (2003) Low-dose CT of the abdomen: evaluation of image improvement with use of noise reduction filters pilot study. Radiology 228:251–256
18. Leipsic J, Nguyen G, Brown J, Sin D, Mayo JR (2010) A prospective evaluation of dose reduction and image quality in chest CT using adaptive statistical iterative reconstruction. AJR Am J Roentgenol 195:1095–1099
19. Prakash P, Kalra MK, Ackman JB et al (2010) Diffuse lung disease: CT of the chest with adaptive statistical iterative reconstruction technique. Radiology 256:261–269
20. Dewes P, Frellesen C, Scholtz J-E et al (2016) Low-dose abdominal computed tomography for detection of urinary stone disease − Impact of additional spectral shaping of the X-ray beam on image quality and dose parameters. Eur J Radiol
21. Gordic S, Morsbach F, Schmidt B et al (2014) Ultralow-dose chest computed tomography for pulmonary nodule detection: first performance evaluation of single energy scanning with spectral shaping. Invest Radiol 49:465–473
22. Huber A, Landau J, Ebner L et al (2016) Performance of ultralow-dose CT with iterative reconstruction in lung cancer screening: limiting radiation exposure to the equivalent of conventional chest X-ray imaging. Eur Radiol 26:3643–3652
23. Deak PD, Smal Y, Kalender WA (2010) Multisection CT protocols: sex- and age-specific conversion factors used to determine effective dose from dose-length product. Radiology 257:158–166
24. Boone J, Strauss K, Cody D (2011) Size-Specific Dose Estimates (SSDE) in Pediatric and Adult Body CT Examinations, Report of AAPM Task Group 204
25. Hansell DM, Bankier AA, MacMahon H, McLoud TC, Muller NL, Remy J (2008) Fleischner Society: glossary of terms for thoracic imaging. Radiology 246:697–722
26. Nagatani Y, Takahashi M, Murata K et al (2015) Lung nodule detection performance in five observers on computed tomography (CT) with adaptive iterative dose reduction using three-dimensional processing (AIDR 3D) in a Japanese multicenter study: Comparison between ultra-low-dose CT and low-dose CT by receiver-operating characteristic analysis. Eur J Radiol 84:1401–1412
27. de Hoop B, van Ginneken B, Gietema H, Prokop M (2012) Pulmonary perifissural nodules on CT scans: rapid growth is not a predictor of malignancy. Radiology 265:611–616
28. Bates D, Martin M, Bolker B, Walker S (2015) Fitting linear mixed-effects models using lme4. J Stat Softw 67(1):1–48
29. Mettler FA Jr, Huda W, Yoshizumi TT, Mahesh M (2008) Effective doses in radiology and diagnostic nuclear medicine: a catalog. Radiology 248:254–263
30. Wahidi MM, Govert JA, Goudar RK, Gould MK, McCrory DC, American College of Chest P (2007) Evidence for the treatment of patients with pulmonary nodules: when is it lung cancer?: ACCP evidence-based clinical practice guidelines (2nd edition). Chest 132:94S–107S
31. Baldwin DR, Callister ME, Guideline Development G (2015) The British Thoracic Society guidelines on the investigation and management of pulmonary nodules. Thorax 70:794–798
32. (2015) Natural Radiation in western Europe. http://www.world-nuclearorg/information-library/safety-and-security/radiation-and-health/naturally-occurring-radioactive-materials-normaspx World Nuclear Association
33. Miglioretti DL, Ichikawa L, Smith RA et al (2015) Criteria for identifying radiologists with acceptable screening mammography interpretive performance on basis of multiple performance measures. AJR Am J Roentgenol 204:W486–W491
34. Martini K, Barth BK, Nguyen-Kim TD, Baumueller S, Alkadhi H, Frauenfelder T (2016) Evaluation of pulmonary nodules and infection on chest CT with radiation dose equivalent to chest radiography: prospective intra-individual comparison study to standard dose CT. Eur J Radiol 85:360–365
35. Barrett JF, Keat N (2004) Artifacts in CT: recognition and avoidance. Radiographics 24:1679–1691